Phospholipase D1 promotes astrocytic differentiation through the FAK/AURKA/STAT3 signaling pathway in hippocampal neural stem/progenitor cells

Min-Jeong Kang
Hanyang University - Seoul Campus: Hanyang University
Nuri Jin
Hanyang University - Seoul Campus: Hanyang University
Shin-Young Park (ttokttoki@hanyang.ac.kr)
Hanyang University https://orcid.org/0000-0002-6073-4634
Joong-Soo Han
Hanyang University Medical School: Hanyang University College of Medicine

Research Article

Keywords: Phospholipase D1, Astrocytic differentiation, Glial fibrillary acidic protein, Hippocampal neural stem/progenitor cells, Phosphatidic acid

Posted Date: June 13th, 2022

DOI: https://doi.org/10.21203/rs.3.rs-1710495/v1

Abstract

Phospholipase D1 (PLD1) plays a crucial role in cell differentiation of different cell types. However, the involvement of PLD1 in astrocytic differentiation remains uncertain. In the present study, we investigate the possible role of PLD1 and its product phosphatidic acid (PA) in astrocytic differentiation of hippocampal neural stem/progenitor cells (NSPCs) from hippocampi of embryonic day 16.5 rat embryos. We showed that overexpression of PLD1 increased the expression level of glial fibrillary acidic protein (GFAP), an astrocyte marker, and the number of GFAP-positive cells. Knockdown of PLD1 by transfection with Pld1 shRNA inhibited astrocytic differentiation. Moreover, PLD1 deletion (*Pld1*$^{-/-}$) suppressed the level of GFAP in the mouse hippocampus. These results indicate that PLD1 plays a crucial role in regulating astrocytic differentiation in hippocampal NSPCs. Interestingly, PA itself was sufficient to promote astrocytic differentiation. PA-induced GFAP expression was decreased by inhibition of signal transducer and activation of transcription 3 (STAT3) using siRNA. Furthermore, PA-induced STAT3 activation and astrocytic differentiation were regulated by the focal adhesion kinase (FAK)/aurora kinase A (AURKA) pathway. Taken together, our findings suggest that PLD1 is an important modulator of astrocytic differentiation in hippocampal NSPCs via the FAK/AURKA/STAT3 signaling pathway.

Introduction

In the development of the central nervous system (CNS), neural stem/progenitor cells (NSPCs) possess the ability to proliferate, self-renew, and produce both neuronal and glial lineages [1, 2]. During forebrain development, neural stem cells generate neurons first, followed by astrocytes and then oligodendrocytes. This temporal sequence of differentiation in the CNS is strictly regulated by both intrinsic programs and extracellular signals [3, 4]. However, the molecular mechanisms by which hippocampal NSPCs undergo differentiation into the distinct cell types are unclear.

Astrocytes are the most abundant type of glial cells in the nervous system, where they impact the function of surrounding neurons in a variety of ways [5, 6]. Astrocytes arise from neural stem cells that also produce neurons and oligodendrocytes [7]. Glial fibrillary acidic protein (GFAP) has been recognized widely as a marker for astrocyte development, as the major intermediate filament protein of mature astrocytes [8, 9]. Differentiation of NSPCs into GFAP-positive mature astrocytes is induced by activation of signal transducer and activator of transcription 3 (STAT3) [10–12]. Therefore, STAT3 activation could be important for astrocytic differentiation in hippocampal NSPCs, but the molecular mechanisms that govern astrogenesis are largely unknown.

Phospholipase D (PLD), an important regulator of lipid metabolism, is a ubiquitous enzyme that catalyzes the hydrolysis of head groups from phospholipids to produce phosphatidic acid (PA) in response to various extracellular stimuli [13, 14]. PA is a lipid second messenger that participates in multiple signaling processes involved in cell proliferation, differentiation, membrane trafficking, hormone response, and cytoskeletal organization [15–17]. Two mammalian PLD isozymes, including PLD1 and PLD2, have been identified in mammalian cells and characterized extensively in most cell types and

tissues [18]. The two isozymes are regulated differently because they possess distinct cellular localization and functions [19]. Recent studies have revealed that PLD1 is important in embryonic and adult brain development and is involved in neurogenesis, establishment of the neural circuit, and dendritic spine morphogenesis [20, 21]. PLD1-deficient mice have delayed brain development and reduced cognitive function [22], which indicates a crucial role of PLD1 in neural development. In addition, we have reported that PLD1 is involved in the neuronal differentiation of rat cortical neural stem cells [23–25] and H19-7 cells [26, 27]. PLD1 is expressed in both neuron and glia cells in the brain [28], but most research has focused on the effects of PLD1 on neurogenesis and not on astrogenesis.

In the present study, we first investigated the role of PLD1 in astrocytic differentiation of hippocampal NSPCs and found that PLD1 overexpression promotes astrocytic differentiation and rescued the astrogenesis defects caused by PLD1 knockdown. We also demonstrated that PA, a product of PLD1, activates the FAK/AURAK/STAT3(Y705) signaling pathway required for astrocytic differentiation, suggesting that PLD1 can promote the astrogenesis of hippocampal NSPCs.

Materials And Methods

Mice

Pld$^{-/-}$ mice were generated as previously described [29]. Heterozygous breeders were crossed to generate WT, heterozygous, and knockout littermates, and genotypes were determined by PCR analysis (Supplementary Fig. 1). All experiments were conducted with 10-week-old male *Pld*$^{-/-}$ mice. All animal experiments were approved by the Institutional Animal Care and Use Committee (IACUC) of Hanyang University (HY-IACUC-20-0233) and were conducted according to relevant guidelines and regulations.

Primary culture of hippocampal neural stem/progenitor cells

All procedures using animals were performed according to the Hanyang University guidelines for the care and use of laboratory animals and were approved by the Institutional Animal Care and Use Committee of Hanyang University (HY-IACUC-18-0028). Pregnant Sprague–Dawley (SD) rats were obtained from Orient Bio Inc. (Seoul, Korea). Whole brains were collected from SD rat embryos at E16.5 (E1 was defined as 12 hours after detection of a vaginal plug). Embryonic hippocampi were mechanically dissected from the brains and placed in ice-cold Ca^{2+}/Mg^{2+}-free HBSS (Gibco), followed by removal of blood vessels and meninges. The hippocampal tissue was incubated with 0.05% trypsin-EDTA at 37°C for 5 – 10 min and dissolved in N2 medium supplemented with 10% (v/v) heat-inactivated FBS. After centrifugation at 200 × g for 5 min, the pelleted cells were gently resuspended in culture medium and plated at 2 × 10^5 cells on 10-cm culture dishes (Nunc A/S, Roskilde, Denmark) precoated with 15 μg/ml poly-L-ornithine (Sigma-Aldrich) and 1 μg/ml fibronectin (Invitrogen) and incubated at 37°C in a 5% CO_2/95% air-humidified incubator. The cells were then cultured for 5 – 6 days in serum-free N2 medium supplemented with 20 ng/ml bFGF. The medium was changed every other day, while the bFGF was supplemented every day to

expand the population of proliferative stem/precursors. Cell clusters generated by stem/precursor cell proliferation were dissociated in 0.05% trypsin-EDTA and plated at 6×10^4 cells per well on coated 24-well plates, 1×10^6 cells per well on coated 6-well, or 2×10^6 cells on coated 6-cm culture dishes. Passage 1 neural stem/precursor cells were used in all experiments.

Construction of small hairpin RNA (shRNA)-expressing vectors and lentivirus production

For PLD1 silencing, the pLB lentiviral vector (Addgene, Cambridge, MA, USA) containing shRNA was constructed using the *Pld1* shRNA target sequences (sense: 5'-GAATTCACATGGCAAGTTAAG-3' and antisense: 5'-CTTAACTTGCCAT GTGAATTC-3'). The annealed oligonucleotide was digested at XhoI and HpaI restriction sites, and the restriction product was inserted into the pLB vector digested with the same restriction enzymes. The final plasmid construct, pLB-*shPld1*-GFP, was verified by sequencing analysis. Lentivirus was produced by co-transfection of control empty shRNA vector or pLB-*shPld1*-GFP with lentiviral packaging plasmids pLP1, pLP2, and pLP/VSVG (Invitrogen) and transfected into 293T cells (ATCC, Manassas, VA, USA) using Lipofectamine 3000 (Invitrogen). Supernatants containing viral particles were harvested 48 h after 293T cell transfection. For viral transduction, prepared hippocampal NSPCs were incubated with the viral suspension (4×10^6 particles/ml) containing polybrene (1 μg/ml; Sigma-Aldrich) for 24 h, followed by transfer to bFGF-supplemented N2 medium.

Transient transfection of hippocampal NSPCs

NSPCs were transfected using an AMAXA Nucleofector™ Kit V (#VCA-1003, AMAXA Biosystems, Köln, Germany) according to the manufacturer's instructions, except for the following modifications. For each nucleofection sample, 5×10^6 cells were centrifuged at 300 × g for 5 min and resuspended in 100 μl of pre-warmed AMAXA Nucleofector solution. Each 100 μl of cell suspension was mixed with either 10 μg of pCMV6-Entry (empty vector) or pCMV6-Entry encoding MycDDK-tagged *rPld1* complementary DNA (cDNA) (pCMV6-Entry-*rPld1*-MycDDK) (#RR213792, OriGene Technologies, Rockville, MD, USA). The DNA-cell suspensions were immediately transferred into AMAXA nucleofection cuvettes and electroporated using the Nucleofector program G-013 in the nucleofection device (Nucleofector I). The pLB vector or pLB-*shPld1*-GFP was introduced into cells for knockdown experiments using the AMAXA Nucleofector Kit V.

RNA interference

For Stat3 knockdown experiments, Stat3 siRNA (5'-CUGUCUUUAGGCUGAUCAU-3', #25125-1) was purchased from Bioneer (Daejeon, Korea). Negative control siRNA (ON-TARGET plus non-targeting pool, #D-001810-10-20) was purchased from Dharmacon (Lafayette, CO, USA). Transient siRNA transfections were performed in 6-well plates by introducing 150 nM Stat3 siRNA or negative control siRNA into cells using Lipofectamine RNAiMAX transfection reagent (Invitrogen), according to the manufacturer's protocol.

RNA extraction and reverse transcription-quantitative polymerase chain reaction (RT-qPCR)

Total RNA was extracted from cultured cells using NucleoZOL reagent (Macherey-Nagel, Düren, Germany). To prepare cDNA by qPCR, purified total RNA (300 ng) was reverse transcribed using GoScript™ Reverse Transcriptase and random primers (Promega Corporation, Madison, WI, USA). The qPCR was performed using a SensiFAST™ SYBR No-ROX Kit (Bioline, London, UK) on a CFX Connect™ Real-Time PCR Detection System (Bio-Rad, Hercules, CA, USA). The primers used for RT-qPCR were as follows: Rat *Gfap* sense: 5'-GAGATCGCCACCTACAGGAA-3' and antisense: 5'-GCTCCTGCTTCGACTCCTTA-3', Rat *Gapdh* sense: 5'-GGCATTGCTCTCAATGACAA-3' and antisense: 5'-AGGGCCTCTCTCTTGCTCTC-3'. Thermocycling conditions were 95°C for 10 min, followed by 40 cycles of 95°C for 15 s and 60°C for 1 min. Each sample was tested in duplicate, and at least three samples obtained from independent experiments were analyzed. Relative quantification was carried out using the $2^{-\Delta\Delta Ct}$ method. Relative gene expression was normalized to the that of the internal control, GAPDH.

Western blot assays

Cells were lysed in ice-cold RIPA lysis buffer (50 mM Tris-HCl pH 7.5, 150 mM NaCl, 0.1% (v/v) NP-40, 0.25% (v/v) sodium deoxycholate) supplemented with 1× Complete EDTA-free Protease Inhibitor Cocktail (Roche Diagnostics, Indianapolis, IN, USA) and 1× Halt™ Phosphatase Inhibitor Cocktail (Thermo Fisher Scientific, Waltham, MA, USA). Protein samples (20–30 µg) were loaded on 8–10% SDS–polyacrylamide gels and then transferred to nitrocellulose membranes (Amersham Pharmacia Biotech, Amersham, UK) after electrophoresis. After blocking with 5% (w/v) non-fat dried milk for 1 h, membranes were incubated with primary antibodies against rabbit polyclonal anti-PLD1 (1:500 dilution), mouse monoclonal anti-GFAP (1:500 dilution), rabbit polyclonal anti-phospho-STAT3 (Tyr 705) (1:1000 dilution), mouse monoclonal anti-STAT3 (1:1000 dilution), mouse monoclonal anti-phospho-AURKA (Thr 288) (1:200 dilution), mouse monoclonal anti-AURKA (1:200 dilution), rabbit polyclonal anti-phospho-FAK (Tyr 397) (1:1000 dilution), rabbit polyclonal anti-FAK (1:1000 dilution), and rabbit polyclonal anti-calnexin antibody (1:2000 dilution), followed by HRP-conjugated secondary antibodies anti-rabbit IgG (#111-035-003) and anti-mouse IgG (#115-035-003) (1:10,000 dilution, Jackson ImmunoResearch, West Grove, PA, USA). Since calnexin is widely used as a house keeping gene [30–32] and is stably expressed in rat hippocampal neural precursor cells in this study, it was used as loading control. Specific bands were detected by an enhanced chemiluminescence western blotting detection system (Thermo Fisher Scientific, Rockford, IL, USA) and were quantified using Quantity One® software (Bio-Rad).

Immunofluorescence on cultured cells

Cells were fixed with 4% (w/v) paraformaldehyde in phosphate-buffered saline (PBS) for 20 min and then washed three times with 0.1% (w/v) BSA in PBS at room temperature. After blocking with 10% (v/v) normal goat serum in 0.1% BSA in PBS containing 0.3% (v/v) Triton X-100 for 1 h at room temperature, cells were immunostained with rabbit polyclonal anti-GFAP primary antibody (1:500 dilution) at 4°C overnight. Subsequently, cells were washed three times with PBS and then labeled with 1:2000 dilution of Alexa Fluor® 594-conjugated goat anti-rabbit IgG (H + L) secondary antibody for 1 h before mounting with Vectashield mounting medium (Vector Laboratories, Burlingame, CA, USA) containing 4,6-diamidino-

2-phenylindole (DAPI). Immunoreactive cells were detected and photographed using an epifluorescence microscope (Nikon Instruments, Melville, NY, USA) at magnifications ranging from 20× to 40×.

Immunofluorescence in tissue sections

Mice were perfused with 4% paraformaldehyde in PBS and processed for histology. Brains were removed and fixed in 4% paraformaldehyde for 24 h at 4°C and embedded in paraffin. For immunofluorescence labeling, serial sections (5 μm/section) were deparaffinized. They were then incubated in 10% normal goat serum (NGS) for 1 h at room temperature for blocking before primary antibody staining. Specimens were stained with mouse monoclonal anti-PLD1 primary antibody (1:100 dilution) or rabbit polyclonal GFAP primary antibody (1:200 dilution) at 4°C overnight. To detect primary antibodies, specimens were incubated for 1 h with 1:1000 dilution of Alexa Fluor® 488-conjugated goat anti-mouse IgG (H + L) secondary antibody or 1:1000 dilution of Alexa Fluor® 594-conjugated goat anti-rabbit IgG (H + L) secondary antibody. After three washes in PBS, they were mounted using Vectashield mounting medium. Images were acquired by confocal microscopy (Leica Microsystems, Wetzlar, Germany).

Cell counting and analysis

Cells were cultured on coverslips in 24-well plates, fixed with 0.1% (w/v) picric acid/PBS containing 4% paraformaldehyde, and incubated overnight at 4°C with an anti-GFAP antibody (1:500 dilution). After incubation with a 1:2000 dilution of Alexa Fluor® 594-conjugated goat anti-rabbit IgG secondary antibody, cells were mounted on slides with Vectashield. Cell counting was performed in a microscopic field, using an eyepiece grid at a final magnification of 200× or 400×. GFAP-positive and DAPI-stained cells were counted in 5–10 (fractionator) microscope fields of each culture slide. For each condition, cells from four slides were stained and counted, and each experiment was repeated at least three times. Photos of the cells were captured with an epifluorescence microscope (Nikon Instruments).

Statistical analysis

Data were statistically analyzed using GraphPad Prism 8.0. The unpaired *t*-test was when comparing two groups. One-way ANOVAs followed by Tukey's multiple comparisons *post hoc* test were used when comparing more than two groups. All quantitative data are expressed as mean ± standard error of the mean (SEM), and values of $p < 0.05$ were considered statistically significant. In each experiment, all measurements were performed at least in triplicate, and data consistency was observed in repeated experiments.

Results

PLD1 increases the expression of GFAP in hippocampal NSPCs

Because astrogenesis initiates and continues during late embryonic development, dissected and mechanically dissociated cells from brain hippocampi of E16.5 rat embryos were used to isolate

hippocampal NSPCs. For growth of these cells, fresh basic fibroblast growth factor bFGF (20 ng/ml) was present to prevent differentiation and promote proliferation. To determine whether PLD1 induces astrocytic differentiation, we first investigated the effects of PLD1 overexpression. Either pCMV6-Entry or pCMV6-Entry-*rPld1*-MycDDK was transiently transfected into the hippocampal NSPCs. Three days after transfection of hippocampal NSPCs with pCMV6-Entry or pCMV6-Entry-*rPld1*-MycDDK, the expression of GFAP, an astrocyte marker, was examined by real-time PCR analyses and western blotting. We showed that mRNA level of *Gfap* (Fig. 1A) and protein expression of GFAP (Fig. 1B and 1C) were significantly increased by PLD1 overexpression in the presence of bFGF compared with the vector control. To confirm whether PLD1 has a modulatory effect on astrocytic differentiation, immunofluorescent analysis was performed using GFAP antibody. Astrocytes were quantified by normalizing the total number of GFAP-positive cells to the total number of DAPI-labeled cell nuclei. As shown in Fig. 1D-E, the percentage composition of astrocytes (GFAP-positive cells) was significantly elevated after transfection with *Pld1* compared to vector control cultures (29.8 ± 4.1% versus 5.7 ± 0.6%, $p < 0.01$), indicating that PLD1 promotes astrocytic differentiation of hippocampal NSPCs.

PLD1 deficiency suppresses astrocytic differentiation of hippocampal NSPCs

To further assess the role of PLD1 in expression of GFAP in hippocampal NSPCs, rescue experiments were performed. To exclude the off-target effects of *Pld1* shRNA, hippocampal NSPCs were co-transfected with shRNA targeting *Pld1* mRNA and plasmid DNA encoding *Pld1* for 3 days. Importantly, the inhibitory effect of *Pld1* shRNA on GFAP expression was fully rescued by exogenous addition of *Pld1*, confirming that PLD1 most likely impacts astrocytic differentiation (Fig. 2A and 2B). Consistently, immunofluorescent staining showed that GFAP-positive cells were rescued (12.5 ± 1.6% versus 3.5 ± 0.9%, $p < 0.01$, Fig. 2C and 2D). To confirm the role of PLD1 in astrocytic differentiation, we used $Pld1^{-/-}$ mice as the *Pld1* knockout, while $Pld1^{+/+}$ littermates were used as the wild-type. As shown in Fig. 3A and 3B, GFAP-positive cells were significantly decreased in the hippocampus of $Pld1^{-/-}$ mice compared to $Pld1^{+/+}$ mice (4.0 ± 1.7% versus 28.7 ± 5.8%, $p < 0.01$). Moreover, we found that PLD1 co-localized with GFAP in the hippocampus of $Pld1^{+/+}$ mice (Fig. 3A) indicating the correlation between PLD1 and GFAP in astrocytic differentiation. Consistent with immunohistochemical staining results, expression level of GFAP was inhibited in the hippocampus of $Pld1^{-/-}$ mice (Fig. 3C and 3D). Taken together, these results indicate that PLD1 is crucial for expression of GFAP and astrocytic differentiation in hippocampal NSPCs.

PA, a PLD1 product, can promote astrocytic differentiation by itself

Mammalian PLD1 displays enzymatic activity, catalyzing the hydrolysis of phosphatidylcholine to produce PA and free choline. Because free choline is not thought to fulfill any intracellular signaling role [33], most of the biological function of PLD1 is thought to be mediated by PA, which is a substrate that generates other signaling or bioactive lipids [34, 35]. To examine whether PA, a PLD1 product, is required

for astrocytic differentiation, we treated cells with a water-soluble synthetic short-chain PA (C8-PA) in a time-dependent manner. PA-mediated signaling can be complicated by further metabolization to diacylglycerol or lysophosphatidic acid in the cells, which would initiate signaling through the membrane-bound lysophosphatidic acid receptors [36]. To rule out potential complications from exogenous PA-derived metabolites, a C8-PA species that would not be converted into active LPA was used and delivered into cells [37]. When we added 100 μM of C8-PA to cells for the indicated time points, the mRNA (Fig. 4A) and protein levels of GFAP (Fig. 4B and 4C) were gradually increased under proliferation conditions. Moreover, GFAP-positive cells were significantly increased in C8-PA-treated cells compared with non-treated cells (36.3 ± 3.8% versus 3.2 ± 1.3%, $p < 0.001$, Fig. 4D and 4E), which is consistent with the overexpression of PLD1 on astrocytic differentiation. These results imply that PLD1 increases astrocytic differentiation through its enzymatic product PA.

STAT3 activation is involved in PA-mediated GFAP expression in hippocampal NSPCs

We next investigated which signaling pathway was responsible for PA-mediated astrocytic differentiation of hippocampal NSPCs. STAT3 is a well-known transcription factor that binds to the GFAP promoter region. Activation of STAT3 can promote astrocytic differentiation of neural stem cells [38]. To determine whether STAT3 associates with PA-induced GFAP expression in hippocampal NSPCs, we first examined the phosphorylation of STAT3 by PA stimulation. As shown in Fig. 5A, PA significantly increased the phosphorylation of STAT3 at Tyr705 residues by addition of PA for 1 day compared to the untreated control. To confirm whether STAT3 contributes to PA-induced GFAP expression, hippocampal NSPCs were transiently transfected with STAT3 siRNA or control siRNA for 2 days and treated with the C8-PA for 1 day. PA-induced STAT3 activation was efficiently attenuated by STAT3 knockdown (Fig. 5B). We further found that PA-induced mRNA expression of *Gfap* (Fig. 5C) and protein level of GFAP (Fig. 5D and 5E) were suppressed by STAT3 siRNA, indicating that PA-induced GFAP expression is dependent on STAT3. Moreover, the number of GFAP-positive cells was markedly decreased by STAT3 knockdown compared with PA-treated cells (14.7 ± 2.3% versus 35.1 ± 1.7%, $p < 0.01$, Fig. 5F and 5G). These results suggest that STAT3 activity is involved in PA-mediated GFAP expression and astrocytic differentiation of hippocampal NSPCs.

AURKA is required for PA-induced STAT3 activation and astrocytic differentiation

As other studies have reported that Aurora Kinase A (AURKA) mediates STAT3 activation [39, 40], we investigated whether PA induces AURKA phosphorylation. We found that PA-mediated AURKA phosphorylation at Thr288 reached the highest level after 24 h treatment (Fig. 6A). To examine whether activation of AURKA is involved in PA-induced STAT3 activation and astrocytic differentiation of hippocampal NSPCs, cells were treated with PA in the presence or absence of AurAi, an AURKA-specific inhibitor. As shown in Fig. 6B – 6D, direct inhibition of AURKA phosphorylation by AurAi strongly suppressed PA-induced AURKA and STAT3 activation. Furthermore, we found that subsequent PA-induced

mRNA expression of *Gfap* (Fig. 6E) and protein level of GFAP (Fig. 6F and 6G) were significantly decreased by AurAi. In addition, AurAi decreased PA-mediated GFAP-positive cells compared with PA-treated cells (18.8 ± 6.2% versus 35.9 ± 4.5%, $p < 0.05$, Fig. 6H and 6I). Taken together, these findings demonstrated that AURKA is implicated in PA-induced STAT3 activation and astrocytic differentiation.

Effects of FAK on PA-induced AURKA/STAT3 activation and astrocytic differentiation

One of the targets of PA is the focal adhesion kinase (FAK) [41], and several studies had revealed that FAK was a critical molecule in astrocyte morphology [42]. Therefore, we examined the effect of FAK activation on the PA-dependent astrocytic differentiation of hippocampal NSPCs. As shown in Fig. 7A, the phosphorylation of FAK (Tyr397) peaked at 1 h after PA stimulation. Next, we studied whether activation of FAK affects the PA-induced signaling cascade (AURKA/STAT3 pathway). Western blot analysis revealed that addition of a FAK-specific inhibitor, PF-573228, before PA stimulation significantly reduced the amount of activated FAK in cells (Fig. 7B and 7C). As shown in Fig. 7D and 7E, PA-induced phosphorylation of AURKA and STAT3 was significantly decreased by PF-573228. These results demonstrated that FAK is an upstream molecule of the AURKA/STAT3 pathway in PA-induced astrocytic differentiation. Moreover, when the cells were pretreated with FAK inhibitor, PA-induced mRNA expression and protein levels of GFAP (Fig. 7F and 7G) were decreased compared with those in PA-treated cells. Furthermore, PA-induced astrocytic differentiation was strongly blocked by PF-573228 (14.4 ± 2.7% versus 43.3 ± 4.4%, $p < 0.001$), indicating that FAK activation is related to PA-induced astrocytic differentiation (Fig. 7H and 7I). These results suggest that PA-induced astrocytic differentiation is regulated by the FAK/AURKA/STAT3 signaling pathway.

Based on above results, we confirmed whether PLD1 has an effect on the FAK/AURKA/STAT3 pathway. Either pCMV6-Entry or pCMV6-Entry-*rPld1*-MycDDK was transiently transfected into the hippocampal NSPCs. After 24 h transfection, we performed western blotting to check the phosphorylation of FAK, AURKA, and STAT3. We showed that the phosphorylation level of FAK, AURKA, and STAT3 was increased by PLD1 overexpression compared with the vector control (Supplementary Fig. 2). The results suggested that PLD1 is required for the FAK/AURKA/STAT3 signaling pathway in hippocampal NSPCs.

Discussion

PLD1 has multiple roles in the brain, including neurite formation and dendritic branching [43, 44, 28, 45]. We have previously shown that PLD1 facilitates synaptogenesis in rat cortical NSPCs and H19-7 cells [23, 27]. Moreover, our previous study demonstrated that PLD1 increases the expression of Bcl-2, resulting in neurite outgrowth during neuronal differentiation of NSPCs [24]. However, the effects of PLD1 on astrocytic differentiation and the molecular mechanisms by which PLD1 regulates astrogenesis have not yet been defined. In the present study, we investigated the potential roles of PLD1 and its product PA in the regulation of astrocytic differentiation in hippocampal NSPCs, and the findings are summarized in Fig. 8.

We observed that PLD1 overexpression significantly augmented the expression of the astrocyte marker GFAP, whereas depletion of PLD1 diminished GFAP expression. In addition, PLD1 overexpression in the presence of *Pld1* shRNA rescued suppressed GFAP expression. Furthermore, PLD1 knockout ($Pld1^{-/-}$) in mice has an effect on GFAP expression in the hippocampus. These results strongly indicate that PLD1 is required for astrocytic differentiation of hippocampal NSPCs. This is supported by a previous study showing that PLD1 is expressed not only in neurons, but also in astrocytes and thus plays a potential role in differentiation of astrocytes [28].

In the developing CNS, STAT3 is a critical transcription factor for regulation of GFAP and astrogenesis. Previous studies have shown that GFAP expression in neural stem cells is dependent on phosphorylation of STAT3 [46–48]. Interestingly, we found that PA enhances STAT3 (Tyr705) phosphorylation. Furthermore, inhibition of STAT3 activation by STAT3 siRNA suppresses the expression of GFAP and GFAP-positive cells induced by PA, indicating that PA-dependent STAT3 activation is essential for astrocytic differentiation. In line with our results, several reports have demonstrated that STAT3 suppression or conditional ablation repressed glial differentiation [38, 49]. Previously, we reported that PA inhibits astrocytic differentiation by regulating the activity of STAT3 in neural stem cells isolated from E14 cerebral cortex which showed opposite results from the current study. Similarly, it has been reported that hippocalcin promotes neuronal differentiation by inhibiting the activity of STAT3 in neural stem cells from the cerebral cortex[25], but it promotes astrocytic differentiation by increasing the activity of STAT3 in neural stem cells from the hippocampus[50]. It is possible that the same gene or factor may have the opposite action depending on the brain region and cell type.

The serine/threonine AURKA mitotic kinase is best known for unlocking the G2/M transition via centrosome maturation [51]. The position of the centrosome is regulated precisely during neurogenesis, migration, and differentiation [52, 53]. Recent reports suggest that inhibition of AURKA blocks STAT3 tyrosine phosphorylation [39]. The current study provides evidence that AURKA activation is required for PA-mediated STAT3 phosphorylation, leading to astrocytic differentiation. FAK has been implicated in regulating cytoskeletal rearrangement in astrocytes [42], and it has been reported that FAK phosphorylation is regulated by PLD [41]. These findings are consistent with our study, which showed that PA-induced GFAP expression was decreased by treatment with an FAK inhibitor. In addition, FAK mediated the activation of the AURAK/STAT3 signaling pathway in PA-induced astrocytic differentiation. Therefore, we suggest that astrogenesis in hippocampal NSPCs is strongly associated with activation of the FAK/AURKA/STAT3 signaling pathway. However, a previous study has shown that AURKA acts as an upstream molecule of FAK phosphorylation [54]. Also to be considered, phosphorylation of FAK by PA treatment increased at 1 h (Fig. 7A), and phosphorylation of AURKA increased at 24 h after treatment with PA (Fig. 6A). The reason for such a time interval is probably that the phosphorylation of FAK by PA did not directly affects phosphorylation of AURKA, and it is possible that other signaling factors were involved. Therefore, it is necessary to discover how FAK affects AURKA activation during PLD1/PA-induced astrocytic differentiation.

Conclusion

Altogether, we demonstrate a novel function of PLD1 in astrocytic differentiation of hippocampal NSPCs. First, we found that PLD1 promotes astrocytic differentiation, and that PA, an enzymatic product of PLD1, mimics the effects of PLD1 on astrogenesis. Second, stimulation with PA leads to an increase of GFAP expression by inducing phosphorylation of STAT3. Third, PA-mediated STAT3 activation occurs through the FAK/AURKA pathway, resulting in astrocytic differentiation. To the best of our knowledge, this is the first report to show that PLD1 and PA promote astrocytic differentiation through a FAK/AURKA/STAT3 pathway in hippocampal NSPCs.

Declarations

Acknowledgements

We thank Prof. Do Sik Min (Yonsei University, Republic of Korea) for providing *pld1*$^{-/-}$ mice.

Author Contributions

MJK was responsible for conception and design, acquisition of data, analysis of data, and drafting or revising the article. NJ helped in mouse experiments. SYP and JSH were responsible for supervising the project, drafting and revising the article, and providing the requested funding. All authors contributed to the article and approved the submitted version.

Funding

This work was supported by a National Research Foundation of Korea (NRF) grant funded by the Korean government (MSIT) (2021R1A2C1008317) and partly supported by the research fund of Hanyang University (HYY-2020).

Data Availability

The datasets used and/or analyzed during the current study are available from the corresponding author upon reasonable request.

Ethics Approval and Consent to Participate

The manuscript does not contain clinical studies or patient data. All animal experiments were approved by the Institutional Animal Care and Use Committee (IACUC) of Hanyang University (HY-IACUC-20-0233 and HY-IACUC-18-0028) and were conducted according to relevant guidelines and regulations.

Consent to Participate

Not applicable

Consent for Publication

Not applicable

Code Availability

Not applicable

Competing Interests

The authors declare that they have no conflict of interest.

References

1. Temple S (2001) The development of neural stem cells. Nature 414(6859):112–117. doi:10.1038/35102174
2. Hirabayashi Y, Gotoh Y (2005) Stage-dependent fate determination of neural precursor cells in mouse forebrain. Neurosci Res 51(4):331–336. doi:10.1016/j.neures.2005.01.004
3. Imayoshi I, Kageyama R (2014) bHLH factors in self-renewal, multipotency, and fate choice of neural progenitor cells. Neuron 82(1):9–23. doi:10.1016/j.neuron.2014.03.018
4. Albert M, Huttner WB (2018) Epigenetic and Transcriptional Pre-patterning-An Emerging Theme in Cortical Neurogenesis. Front Neurosci 12:359. doi:10.3389/fnins.2018.00359
5. Lopez-Hidalgo M, Schummers J (2014) Cortical maps: a role for astrocytes? Curr Opin Neurobiol 24(1):176–189. doi:10.1016/j.conb.2013.11.001
6. Clarke LE, Barres BA (2013) Emerging roles of astrocytes in neural circuit development. Nat Rev Neurosci 14(5):311–321. doi:10.1038/nrn3484
7. Merkle FT, Alvarez-Buylla A (2006) Neural stem cells in mammalian development. Curr Opin Cell Biol 18(6):704–709. doi:10.1016/j.ceb.2006.09.008
8. Yang Z, Wang KK (2015) Glial fibrillary acidic protein: from intermediate filament assembly and gliosis to neurobiomarker. Trends Neurosci 38(6):364–374. doi:10.1016/j.tins.2015.04.003
9. Messing A, Brenner M (2020) GFAP at 50. ASN Neuro 12:1759091420949680. doi:10.1177/1759091420949680
10. Bonni A, Sun Y, Nadal-Vicens M, Bhatt A, Frank DA, Rozovsky I, Stahl N, Yancopoulos GD, Greenberg ME (1997) Regulation of gliogenesis in the central nervous system by the JAK-STAT signaling pathway. Science 278(5337):477–483
11. Nakashima K, Yanagisawa M, Arakawa H, Kimura N, Hisatsune T, Kawabata M, Miyazono K, Taga T (1999) Synergistic signaling in fetal brain by STAT3-Smad1 complex bridged by p300. Science 284(5413):479–482. doi:10.1126/science.284.5413.479
12. Takizawa T, Yanagisawa M, Ochiai W, Yasukawa K, Ishiguro T, Nakashima K, Taga T (2001) Directly linked soluble IL-6 receptor-IL-6 fusion protein induces astrocyte differentiation from neuroepithelial

cells via activation of STAT3. Cytokine 13(5):272–279. doi:10.1006/cyto.2000.0831

13. Exton JH (1999) Regulation of phospholipase D. Biochim Biophys Acta 1439(2):121–133. doi:10.1016/s1388-1981(99)00089-x
14. Frohman MA, Sung TC, Morris AJ (1999) Mammalian phospholipase D structure and regulation. Biochim Biophys Acta 1439(2):175–186. doi:10.1016/s1388-1981(99)00093-1
15. Wang X, Devaiah SP, Zhang W, Welti R (2006) Signaling functions of phosphatidic acid. Prog Lipid Res 45(3):250–278. doi:10.1016/j.plipres.2006.01.005
16. Liu Y, Su Y, Wang X (2013) Phosphatidic acid-mediated signaling. Adv Exp Med Biol 991:159–176. doi:10.1007/978-94-007-6331-9_9
17. Brown HA, Thomas PG, Lindsley CW (2017) Targeting phospholipase D in cancer, infection and neurodegenerative disorders. Nat Rev Drug Discov 16(5):351–367. doi:10.1038/nrd.2016.252
18. Gomez-Cambronero J, Keire P (1998) Phospholipase D: a novel major player in signal transduction. Cell Signal 10(6):387–397. doi:10.1016/s0898-6568(97)00197-6
19. Peng X, Frohman MA (2012) Mammalian phospholipase D physiological and pathological roles. Acta Physiol (Oxf) 204(2):219–226. doi:10.1111/j.1748-1716.2011.02298.x
20. Park SY, Han JS (2018) Phospholipase D1 Signaling: Essential Roles in Neural Stem Cell Differentiation. J Mol Neurosci 64(3):333–340. doi:10.1007/s12031-018-1042-1
21. Luo LD, Li G, Wang Y (2017) PLD1 promotes dendritic spine development by inhibiting ADAM10-mediated N-cadherin cleavage. Sci Rep 7(1):6035. doi:10.1038/s41598-017-06121-2
22. Burkhardt U, Stegner D, Hattingen E, Beyer S, Nieswandt B, Klein J (2014) Impaired brain development and reduced cognitive function in phospholipase D-deficient mice. Neurosci Lett 572:48–52. doi:10.1016/j.neulet.2014.04.052
23. Yoon MS, Yon C, Park SY, Oh DY, Han AH, Kim DS, Han JS (2005) Role of phospholipase D1 in neurite outgrowth of neural stem cells. Biochem Biophys Res Commun 329(3):804–811. doi:10.1016/j.bbrc.2005.02.087
24. Park SY, Ma W, Yoon SN, Kang MJ, Han JS (2015) Phospholipase D1 increases Bcl-2 expression during neuronal differentiation of rat neural stem cells. Mol Neurobiol 51(3):1089–1102. doi:10.1007/s12035-014-8773-y
25. Park SY, Yoon SN, Kang MJ, Lee Y, Jung SJ, Han JS (2017) Hippocalcin Promotes Neuronal Differentiation and Inhibits Astrocytic Differentiation in Neural Stem Cells. Stem Cell Reports 8(1):95–111. doi:10.1016/j.stemcr.2016.11.009
26. Oh DY, Park SY, Cho JH, Lee KS, Min do S, Han JS (2007) Phospholipase D1 activation through Src and Ras is involved in basic fibroblast growth factor-induced neurite outgrowth of H19-7 cells. J Cell Biochem 101(1):221–234. doi:10.1002/jcb.21166
27. Yoon SN, Kim KS, Cho JH, Ma W, Choi HJ, Kwon SJ, Han JS (2012) Phospholipase D1 mediates bFGF-induced Bcl-2 expression leading to neurite outgrowth in H19-7 cells. Biochem J 441(1):407–416. doi:10.1042/BJ20110302

28. Klein J (2005) Functions and pathophysiological roles of phospholipase D in the brain. J Neurochem 94(6):1473–1487. doi:10.1111/j.1471-4159.2005.03315.x
29. Dall'Armi C, Hurtado-Lorenzo A, Tian H, Morel E, Nezu A, Chan RB, Yu WH, Robinson KS, Yeku O, Small SA, Duff K, Frohman MA, Wenk MR, Yamamoto A, Di Paolo G (2010) The phospholipase D1 pathway modulates macroautophagy. Nat Commun 1:142. doi:10.1038/ncomms1144
30. Buffolo F, Petrosino V, Albini M, Moschetta M, Carlini F, Floss T, Kerlero de Rosbo N, Cesca F, Rocchi A, Uccelli A, Benfenati F (2021) Neuroinflammation induces synaptic scaling through IL-1beta-mediated activation of the transcriptional repressor REST/NRSF. Cell Death Dis 12(2):180. doi:10.1038/s41419-021-03465-6
31. Goh KJ, Chen JH, Rocha N, Semple RK (2020) Human pluripotent stem cell-based models suggest preadipocyte senescence as a possible cause of metabolic complications of Werner and Bloom Syndromes. Sci Rep 10(1):7490. doi:10.1038/s41598-020-64136-8
32. Park SY, Kang MJ, Han JS (2018) Interleukin-1 beta promotes neuronal differentiation through the Wnt5a/RhoA/JNK pathway in cortical neural precursor cells. Mol Brain 11(1):39. doi:10.1186/s13041-018-0383-6
33. Pelech SL, Vance DE (1984) Regulation of phosphatidylcholine biosynthesis. Biochim Biophys Acta 779(2):217–251. doi:10.1016/0304-4157(84)90010-8
34. Selvy PE, Lavieri RR, Lindsley CW, Brown HA (2011) Phospholipase D: enzymology, functionality, and chemical modulation. Chem Rev 111(10):6064–6119. doi:10.1021/cr200296t
35. Cockcroft S (2009) Phosphatidic acid regulation of phosphatidylinositol 4-phosphate 5-kinases. Biochim Biophys Acta 1791(9):905–912. doi:10.1016/j.bbalip.2009.03.007
36. Billon-Denis E, Tanfin Z, Robin P (2008) Role of lysophosphatidic acid in the regulation of uterine leiomyoma cell proliferation by phospholipase D and autotaxin. J Lipid Res 49(2):295–307. doi:10.1194/jlr.M700171-JLR200
37. Fischer DJ, Nusser N, Virag T, Yokoyama K, Wang D, Baker DL, Bautista D, Parrill AL, Tigyi G (2001) Short-chain phosphatidates are subtype-selective antagonists of lysophosphatidic acid receptors. Mol Pharmacol 60(4):776–784
38. Sun Y, Nadal-Vicens M, Misono S, Lin MZ, Zubiaga A, Hua X, Fan G, Greenberg ME (2001) Neurogenin promotes neurogenesis and inhibits glial differentiation by independent mechanisms. Cell 104(3):365–376. doi:10.1016/s0092-8674(01)00224-0
39. Santo L, Hideshima T, Cirstea D, Bandi M, Nelson EA, Gorgun G, Rodig S, Vallet S, Pozzi S, Patel K, Unitt C, Squires M, Hu Y, Chauhan D, Mahindra A, Munshi NC, Anderson KC, Raje N (2011) Antimyeloma activity of a multitargeted kinase inhibitor, AT9283, via potent Aurora kinase and STAT3 inhibition either alone or in combination with lenalidomide. Clin Cancer Res 17(10):3259–3271. doi:10.1158/1078-0432.CCR-10-3012
40. Katsha A, Arras J, Soutto M, Belkhiri A, El-Rifai W (2014) AURKA regulates JAK2-STAT3 activity in human gastric and esophageal cancers. Mol Oncol 8(8):1419–1428. doi:10.1016/j.molonc.2014.05.012

41. Mahankali M, Henkels KM, Speranza F, Gomez-Cambronero J (2015) A non-mitotic role for Aurora kinase A as a direct activator of cell migration upon interaction with PLD, FAK and Src. J Cell Sci 128(3):516–526. doi:10.1242/jcs.157339
42. Kong M, Munoz N, Valdivia A, Alvarez A, Herrera-Molina R, Cardenas A, Schneider P, Burridge K, Quest AF, Leyton L (2013) Thy-1-mediated cell-cell contact induces astrocyte migration through the engagement of alphaVbeta3 integrin and syndecan-4. Biochim Biophys Acta 1833(6):1409–1420. doi:10.1016/j.bbamcr.2013.02.013
43. Guizzetti M, Moore NH, Giordano G, Costa LG (2008) Modulation of neuritogenesis by astrocyte muscarinic receptors. J Biol Chem 283(46):31884–31897. doi:10.1074/jbc.M801316200
44. Kanaho Y, Funakoshi Y, Hasegawa H (2009) Phospholipase D signalling and its involvement in neurite outgrowth. Biochim Biophys Acta 1791(9):898–904. doi:10.1016/j.bbalip.2009.03.010
45. Zhu YB, Gao W, Zhang Y, Jia F, Zhang HL, Liu YZ, Sun XF, Yin Y, Yin DM (2016) Astrocyte-derived phosphatidic acid promotes dendritic branching. Sci Rep 6:21096. doi:10.1038/srep21096
46. Herrmann JE, Imura T, Song B, Qi J, Ao Y, Nguyen TK, Korsak RA, Takeda K, Akira S, Sofroniew MV (2008) STAT3 is a critical regulator of astrogliosis and scar formation after spinal cord injury. J Neurosci 28(28):7231–7243. doi:10.1523/JNEUROSCI.1709-08.2008
47. Yokogami K, Wakisaka S, Avruch J, Reeves SA (2000) Serine phosphorylation and maximal activation of STAT3 during CNTF signaling is mediated by the rapamycin target mTOR. Curr Biol 10(1):47–50. doi:10.1016/s0960-9822(99)00268-7
48. He F, Ge W, Martinowich K, Becker-Catania S, Coskun V, Zhu W, Wu H, Castro D, Guillemot F, Fan G, de Vellis J, Sun YE (2005) A positive autoregulatory loop of Jak-STAT signaling controls the onset of astrogliogenesis. Nat Neurosci 8(5):616–625. doi:10.1038/nn1440
49. Natarajan R, Singal V, Benes R, Gao J, Chan H, Chen H, Yu Y, Zhou J, Wu P (2014) STAT3 modulation to enhance motor neuron differentiation in human neural stem cells. PLoS ONE 9(6):e100405. doi:10.1371/journal.pone.0100405
50. Kang MJ, Park SY, Han JS (2016) Hippocalcin Is Required for Astrocytic Differentiation through Activation of Stat3 in Hippocampal Neural Precursor Cells. Front Mol Neurosci 9:110. doi:10.3389/fnmol.2016.00110
51. Li S, Deng Z, Fu J, Xu C, Xin G, Wu Z, Luo J, Wang G, Zhang S, Zhang B, Zou F, Jiang Q, Zhang C (2015) Spatial Compartmentalization Specializes the Function of Aurora A and Aurora B. J Biol Chem 290(28):17546–17558. doi:10.1074/jbc.M115.652453
52. Nigg EA, Raff JW (2009) Centrioles, centrosomes, and cilia in health and disease. Cell 139(4):663–678. doi:10.1016/j.cell.2009.10.036
53. Bettencourt-Dias M, Glover DM (2007) Centrosome biogenesis and function: centrosomics brings new understanding. Nat Rev Mol Cell Biol 8(6):451–463. doi:10.1038/nrm2180
54. Wu J, Yang L, Shan Y, Cai C, Wang S, Zhang H (2016) AURKA promotes cell migration and invasion of head and neck squamous cell carcinoma through regulation of the AURKA/Akt/FAK signaling pathway. Oncol Lett 11(3):1889–1894. doi:10.3892/ol.2016.4110

Figures

Fig.1

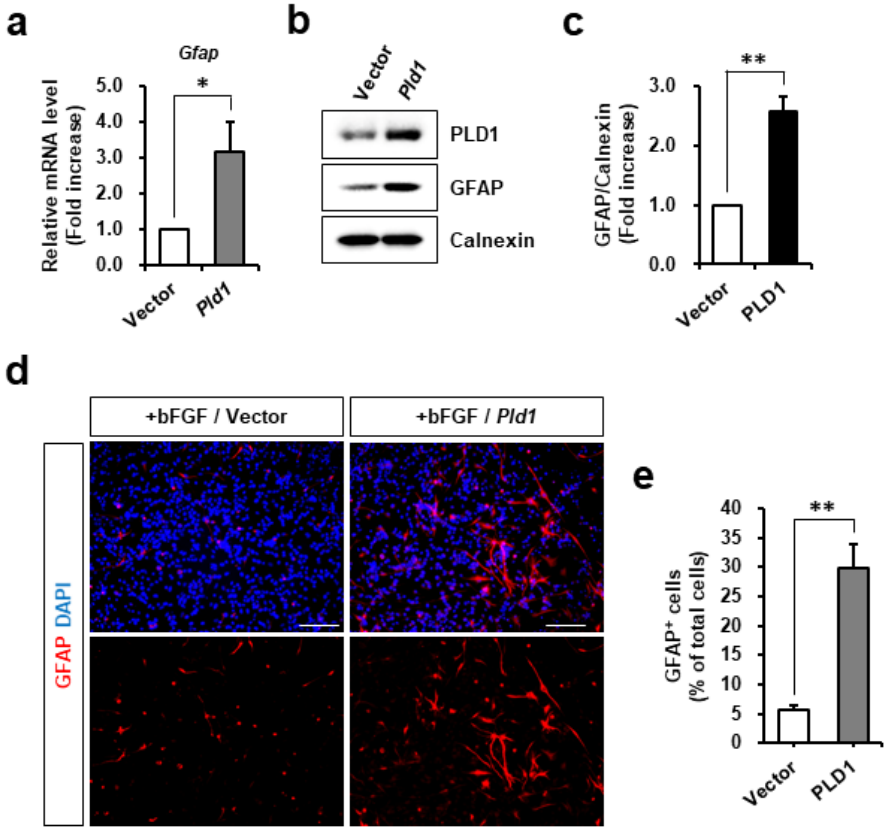

Figure 1

Effect of PLD1 on astrocytic differentiation of hippocampal NSPCs.

(A–C) Hippocampal NSPCs were transiently transfected with pCMV6-Entry (empty vector) or pCMV6-Entry encoding MycDDK-tagged *rPld1* cDNA (pCMV6-Entry-*rPld1*-MycDDK) for 72 h in the presence of bFGF. **(A)** The mRNA level of the astrocyte marker glial fibrillary acidic protein (*Gfap*) was quantitated by real-time RT-PCR. Data represent the mean ± SEM of four independent experiments. *$p < 0.05$ compared with the +bFGF/vector control. (**B)** Proteins were analyzed by western blotting with anti-PLD1, anti-GFAP, and anti-calnexin antibodies. **(C)** Quantitative analyses of the GFAP level shown in (**B)**. GFAP protein level was normalized to the levels of calnexin. Band intensities were quantified using Quantity One® software. Data represent mean ± SEM of three independent experiments. **$p < 0.01$ compared with the vector control. (**D-E)** Cells were transfected with pCMV6-Entry or pCMV6-Entry-*rPld1*-MycDDK for 72 h. **(D)** Fixed cells were immunostained with an anti-GFAP antibody (red) and DAPI (blue). Scale bar, 100 μm. **(E)** The proportions of GFAP-positive cells and total cells were determined in randomly selected areas from five slides of each condition. Data are mean ± SEM. **$p < 0.01$ compared with the vector control.

Fig.2

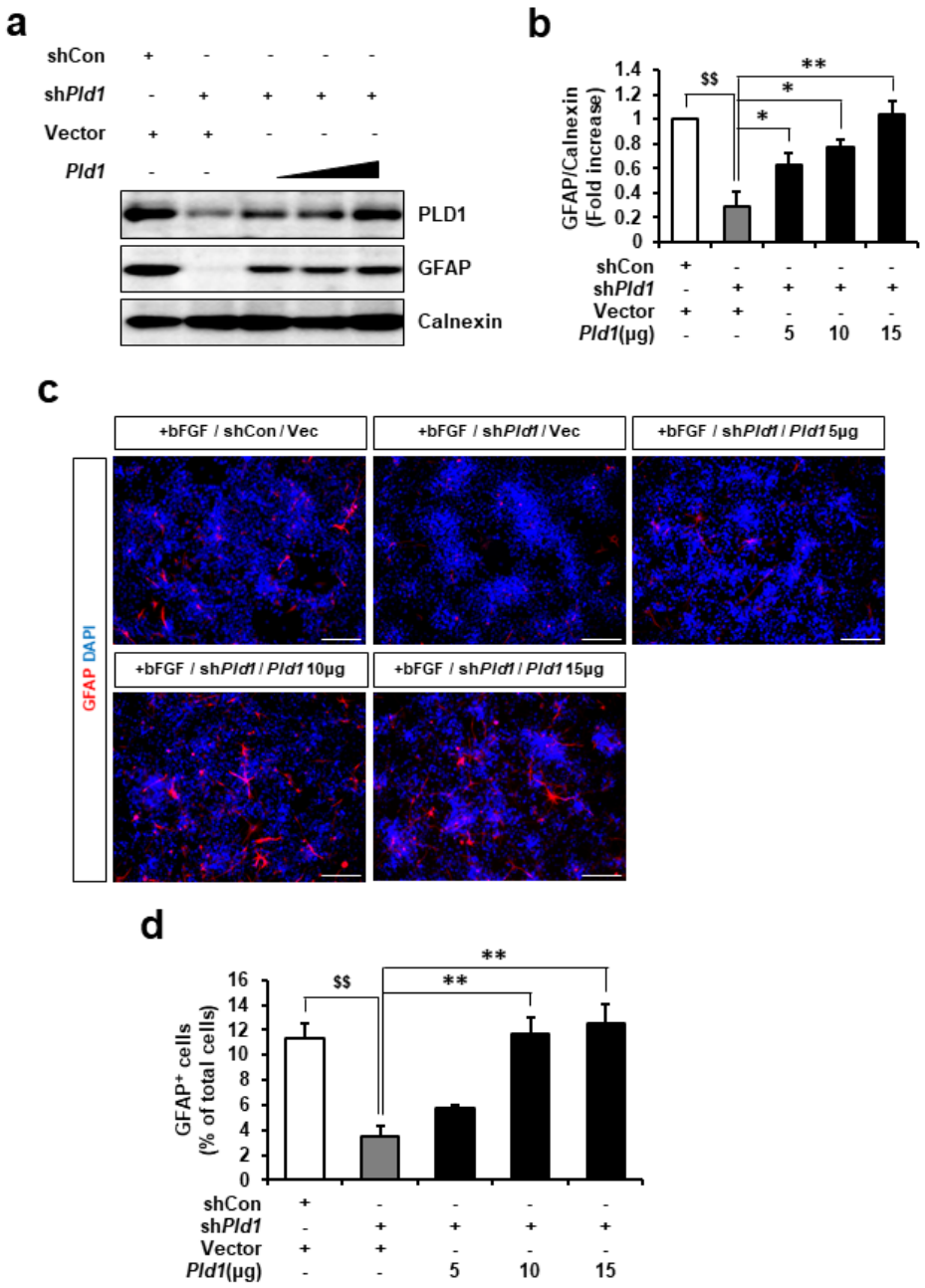

Figure 2

Effect of PLD1 overexpression on astrocytic differentiation of hippocampal NSPCs in the presence of Pld1 shRNA.

(A-B) Control shRNA or *Pld1* shRNA was co-transfected with pCMV6-Entry or pCMV6-Entry-*rPld1*-MycDDK at various doses (0, 5, 10, 15 μg) into hippocampal NSPCs for 72 h. **(A)** Samples containing 30 μg of

protein were analyzed by 10% SDS–PAGE followed by western blotting using anti-PLD1, anti-GFAP, and anti-calnexin antibodies. (**B)** Quantitative analyses of the GFAP levels shown in **(A)**. GFAP protein level was normalized to the level of calnexin. Band intensities were quantified using Quantity One® software. Data represent the mean ± SEM of three independent experiments. $^{\$\$}p < 0.01$ compared with the control shRNA/vector control, $^{*}p < 0.05$, $^{**}p < 0.01$ compared with the *Pld1* shRNA/vector control. (**C-D)** Cells were co-transfected with *Pld1* shRNA and with pCMV6-Entry-*rPld1*-MycDDK at various doses (0, 5, 10, 15 μg) for 72 h. **(C)** The cells were stained with an anti-GFAP antibody (red) and DAPI (blue). Scale bar, 100 μm. **(D)** The numbers of GFAP-positive cells, and total cells were counted in randomly selected areas from five slides of each condition. Data are mean ± SEM. $^{\$\$}p < 0.01$ compared with the control shRNA/vector control, $^{**}p < 0.01$ compared with the *Pld1* shRNA/vector control.

Fig.3

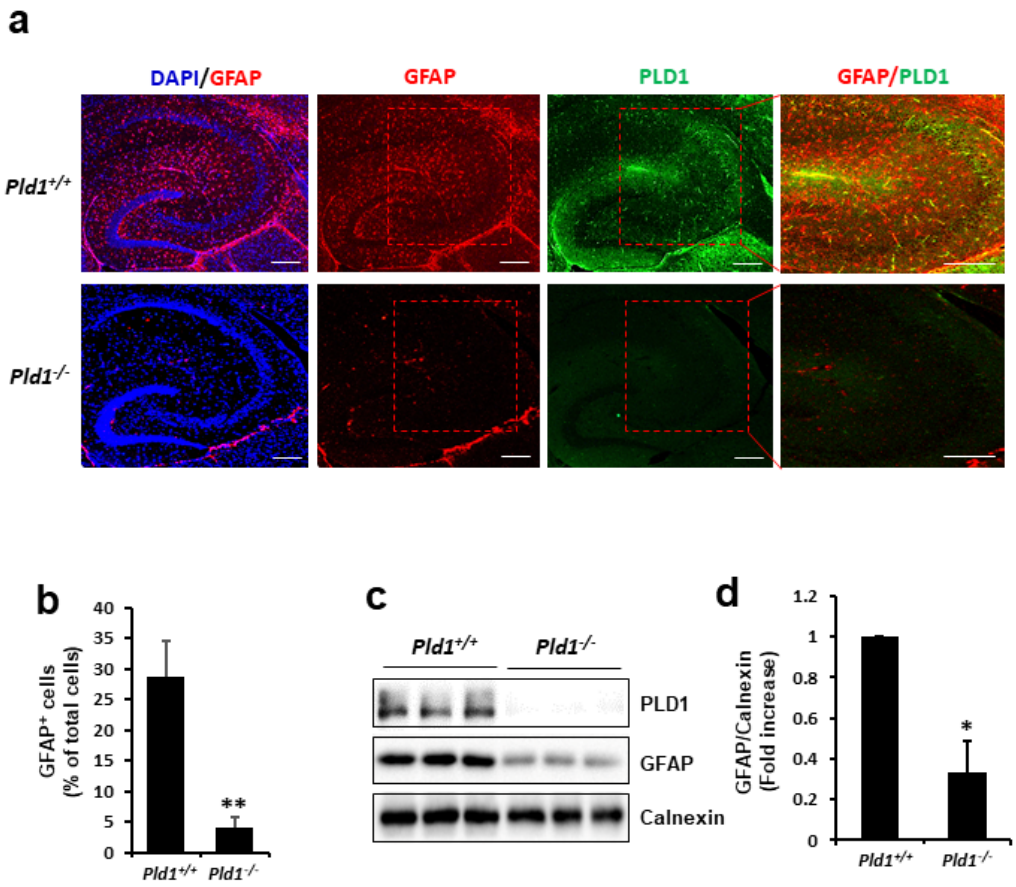

Figure 3

Reduced level of GFAP in the hippocampus of Pld$^{-/-}$ mice.

(A) Immunofluorescent detection of endogenous GFAP (red) and PLD1 (green) in hippocampus sections from *Pld1*$^{+/+}$ and *Pld1*$^{-/-}$ mice. Sections were counterstained with DAPI. The dotted box area is magnified. Scale bar, 50 μm. **(B)** The numbers of GFAP-positive cells and total cells in the hippocampus were

counted in randomly selected areas from five slides of each condition. Data are mean ± SEM. $^{**}p < 0.01$ compared with the *Pld1*$^{+/+}$ mice. **(C)** Representative western blot of PLD1 and GFAP in hippocampus from *Pld1*$^{+/+}$ and *Pld1*$^{-/-}$ mice. **(D)** Quantitative analyses of the GFAP level shown in **(C)**. GFAP protein level was normalized to the level of calnexin. Band intensities were quantified using Quantity One® software. The data are presented as mean ± SEM of three independent experiments. $^{*}p < 0.05$ compared with *Pld1*$^{+/+}$ mice.

Fig.4

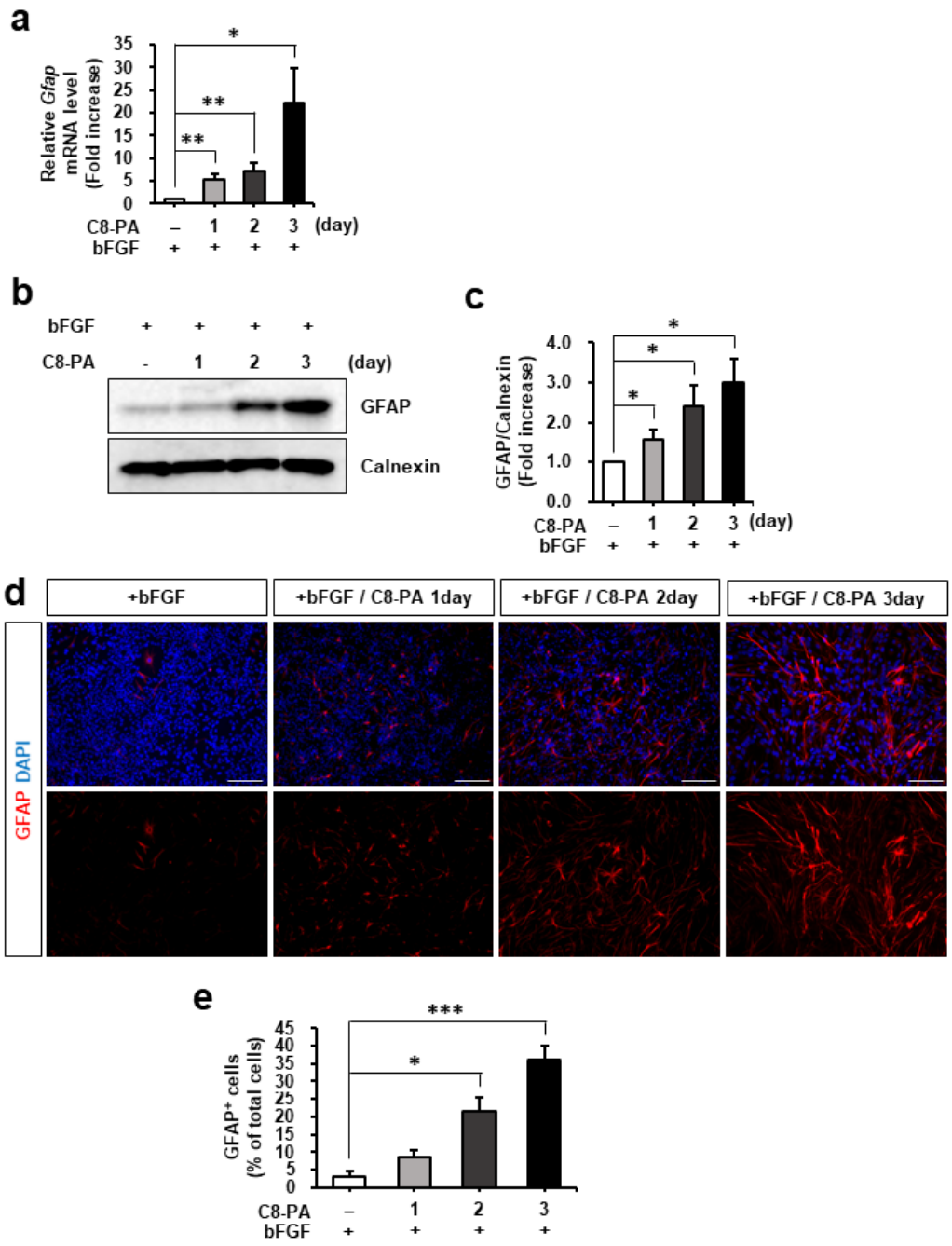

Figure 4

Effect of C8-PA on astrocytic differentiation of hippocampal NSPCs.

(A-C) Hippocampal NSPCs were treated with C8-PA (100 μM) for the indicated time durations in the presence of bFGF. **(A)** *Gfap* mRNA level was analyzed by real-time RT-PCR. Data represent the mean ± SEM of five independent experiments. *$p < 0.05$, **$p < 0.01$ compared with the 0-day control. **(B)** Cells were lysed and analyzed by western blotting with anti-GFAP and anti-calnexin antibodies. (**C)** Quantitative analyses of the GFAP level shown in **(B)**. GFAP protein level was normalized to that of calnexin. Band intensities were quantified using Quantity One® software. Data represent mean ± SEM of three independent experiments. *$p < 0.05$ compared with the untreated control. (**D-E)** Cells were stimulated with C8-PA (100 μM) for the indicated time points. **(D)** Fixed cells were stained with an anti-GFAP antibody (red) and DAPI (blue). Scale bar, 100 μm. **(E)** The numbers of GFAP-positive cells and total cells were counted in randomly selected areas from five slides of each condition. Data are mean ± SEM. *$p < 0.05$, ***$p < 0.001$ compared with the untreated control.

Fig.5

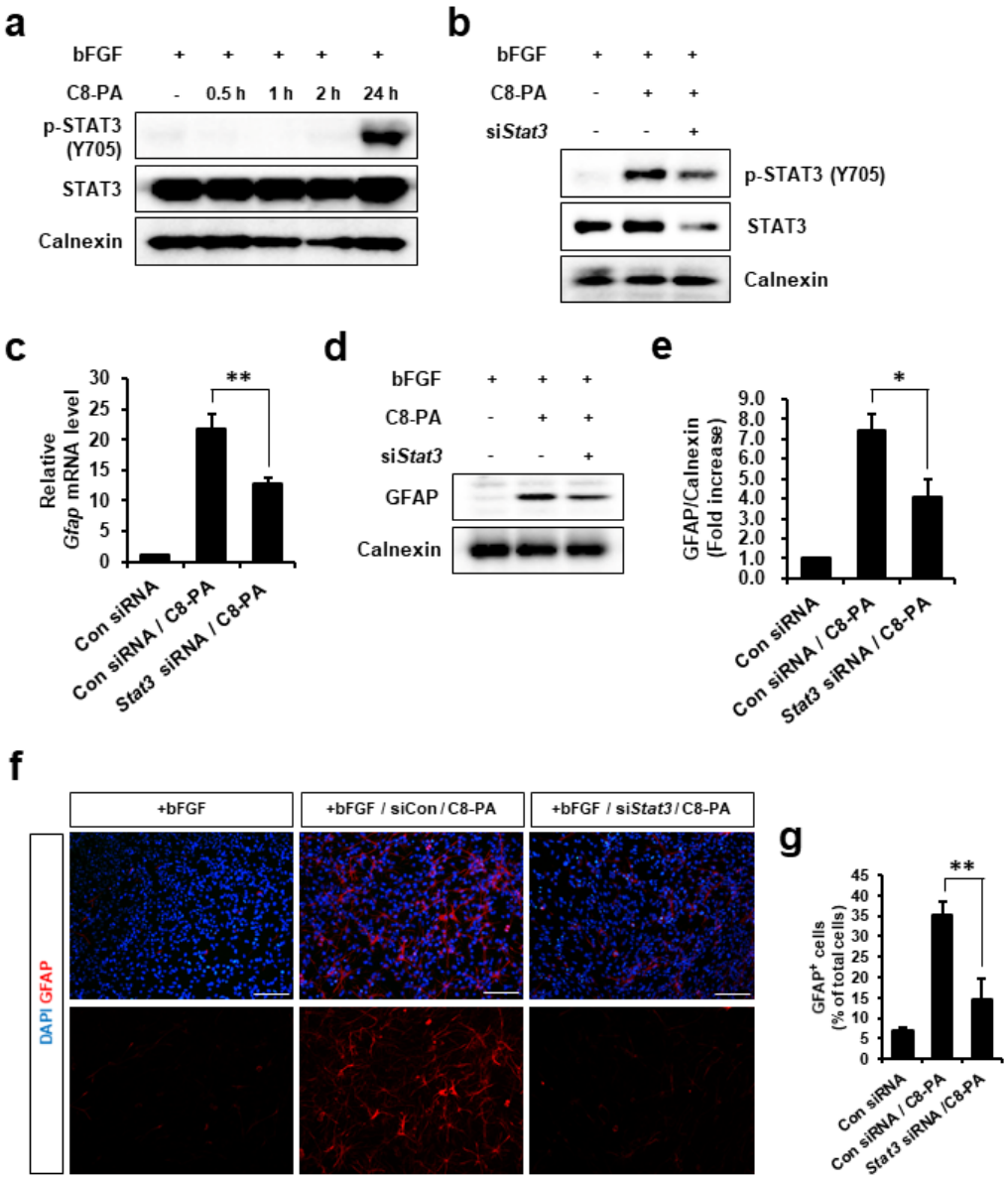

Figure 5

Effect of STAT3 on PA-induced astrocytic differentiation of hippocampal NSPCs.

(A) Hippocampal NSPCs were treated with C8-PA (100 μM) for the indicated time durations in the presence of bFGF, lysed, and harvested. Western blotting was performed using anti-phospho-STAT3 (Tyr705), anti-STAT3, and anti-calnexin antibodies to detect the respective protein bands. **(B)**

Hippocampal NSPCs were transiently transfected with control siRNA or *Stat3* siRNA for 48 h and then treated with C8-PA (100 μM) for 24 h. Cells were lysed and analyzed by western blotting with anti-phospho-STAT3 (Tyr705), anti-STAT3, and anti-calnexin antibodies. **(C-E)** Cells were transfected with control siRNA or *Stat3* siRNA for 48 h and then stimulated with C8-PA (100 μM) for 72 h. **(C)** The mRNA level of *Gfap* was detected by real-time RT-PCR. Data represent the mean ± SEM of three independent experiments. $^{**}p < 0.01$ compared with the control siRNA/C8-PA. **(D)** GFAP protein levels were determined by western blotting. **(E)** Quantitative analyses of the GFAP levels shown in **(D)**. GFAP protein level was normalized to that of calnexin. Band intensities were quantified using Quantity One® software. Data represent the mean ± SEM of three independent experiments. $^{*}p < 0.05$ compared with the control siRNA/C8-PA. (**F-G)** Hippocampal NSPCs were transiently transfected with control siRNA or *Stat3* siRNA for 48 h and then treated with C8-PA (100 μM) for 72 h. **(F)** Fixed cells were stained for immunocytochemical analysis of astrocytic (GFAP, red) markers. Scale bar, 100 μm. **(G)** The proportions of GFAP-positive cells and total cells were determined in randomly selected areas from five slides of each condition. Data are mean ± SEM. $^{**}p < 0.01$ compared with the control siRNA/C8-PA.

Fig.6

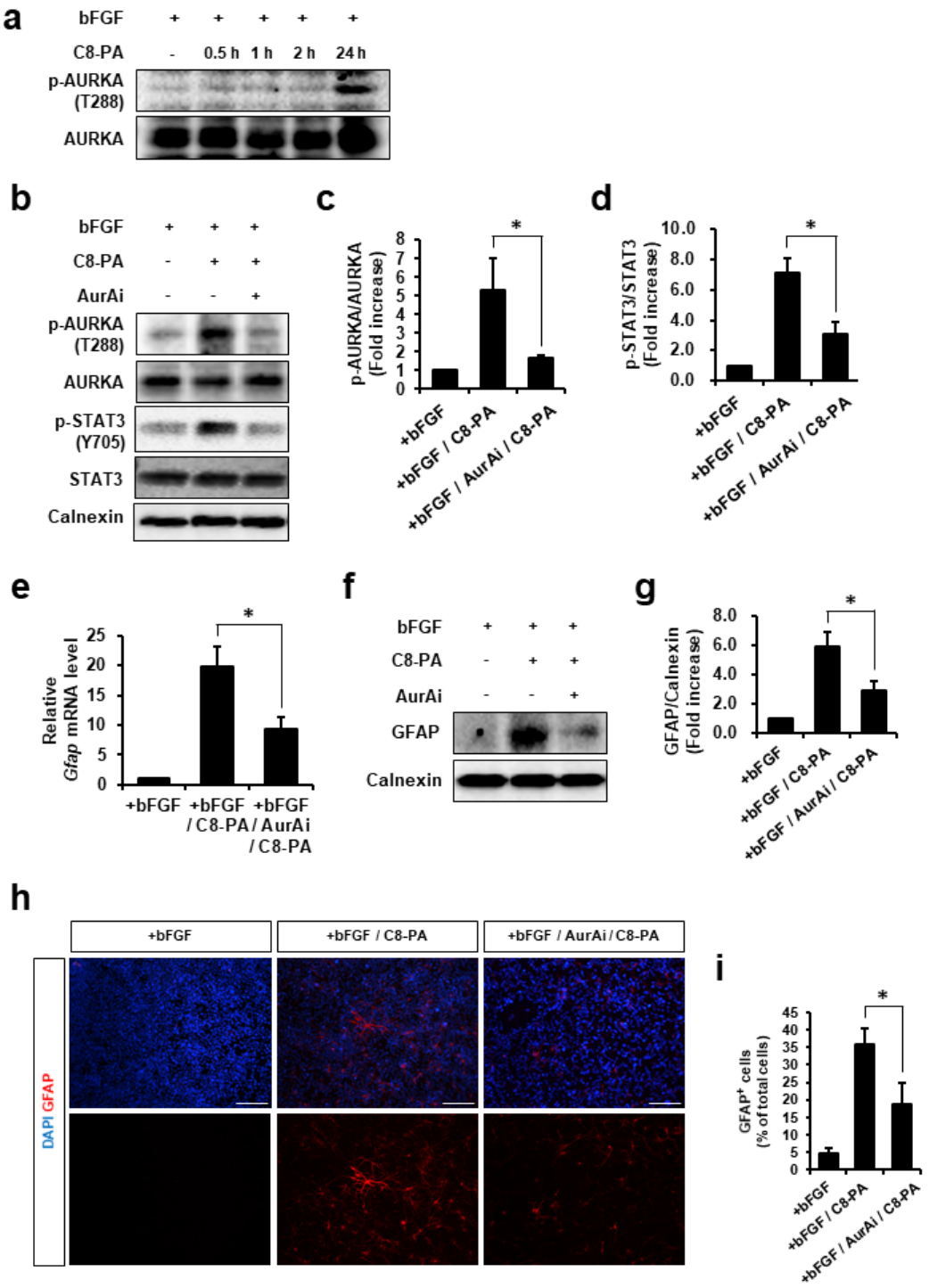

Figure 6

Effects of AURKA on STAT3 activation and PA-induced astrocytic differentiation of hippocampal NSPCs.

(A) Hippocampal NSPCs were stimulated with C8-PA (100 μM) for the indicated time durations in the presence of bFGF. Samples containing 30 μg of protein were analyzed by western blotting using anti-phospho-AURKA (Thr288) antibody and anti-AURKA antibody. (**B-D)** Hippocampal NSPCs were pretreated

with 0.5 μM Aurora A-specific inhibitor (AurAi) for 2 h and treated with C8-PA (100 μM) for 24 h. **(B)** Cell lysates were analyzed by western blotting using anti-phospho-AURKA (Thr288), anti-AURKA, anti-phospho-STAT3 (Tyr705), anti-STAT3, and anti-calnexin antibodies to detect the respective protein bands. **(C-D)** Quantitative analyses of the phospho-AURKA (Thr288) and phosphor-STAT3 (Tyr705) levels shown in **(B)**. Values were normalized to that of the total AURKA or STAT3 level. Band intensities were quantified using Quantity One® software. Data represent the mean ± SEM of three independent experiments. *p < 0.05 compared with the +bFGF/C8-PA. **(E-G)** Cells were pretreated with 0.5 μM AurAi for 2 h and stimulated with C8-PA (100 μM) for 72 h. **(E)** *Gfap* mRNA level was measured by real-time RT-PCR. Data represent the mean ± SEM of four independent experiments. *p < 0.05 compared with C8-PA-treated cells. **(F)** Proteins (20 μg) were analyzed by 10% SDS–PAGE followed by western blotting using anti-GFAP and anti-calnexin antibodies. **(G)** Quantitative analyses of the GFAP levels shown in **(F)**. GFAP protein level was normalized to that of calnexin. Band intensities were quantified using Quantity One® software. Data represent the mean ± SEM of four independent experiments. *p < 0.05 compared with the +bFGF/C8-PA. **(H-I)** Hippocampal NSPCs were pretreated with 0.5 μM AurAi for 2 h and stimulated with C8-PA (100 μM) for 72 h. **(H)** The cells were stained with an anti-GFAP antibody (red) and DAPI (blue). Scale bar, 100 μm. **(I)** The numbers of GFAP-positive cells and total cells were counted in randomly selected areas from five slides of each condition. Data are mean ± SEM. *p < 0.05 compared with the +bFGF/C8-PA.

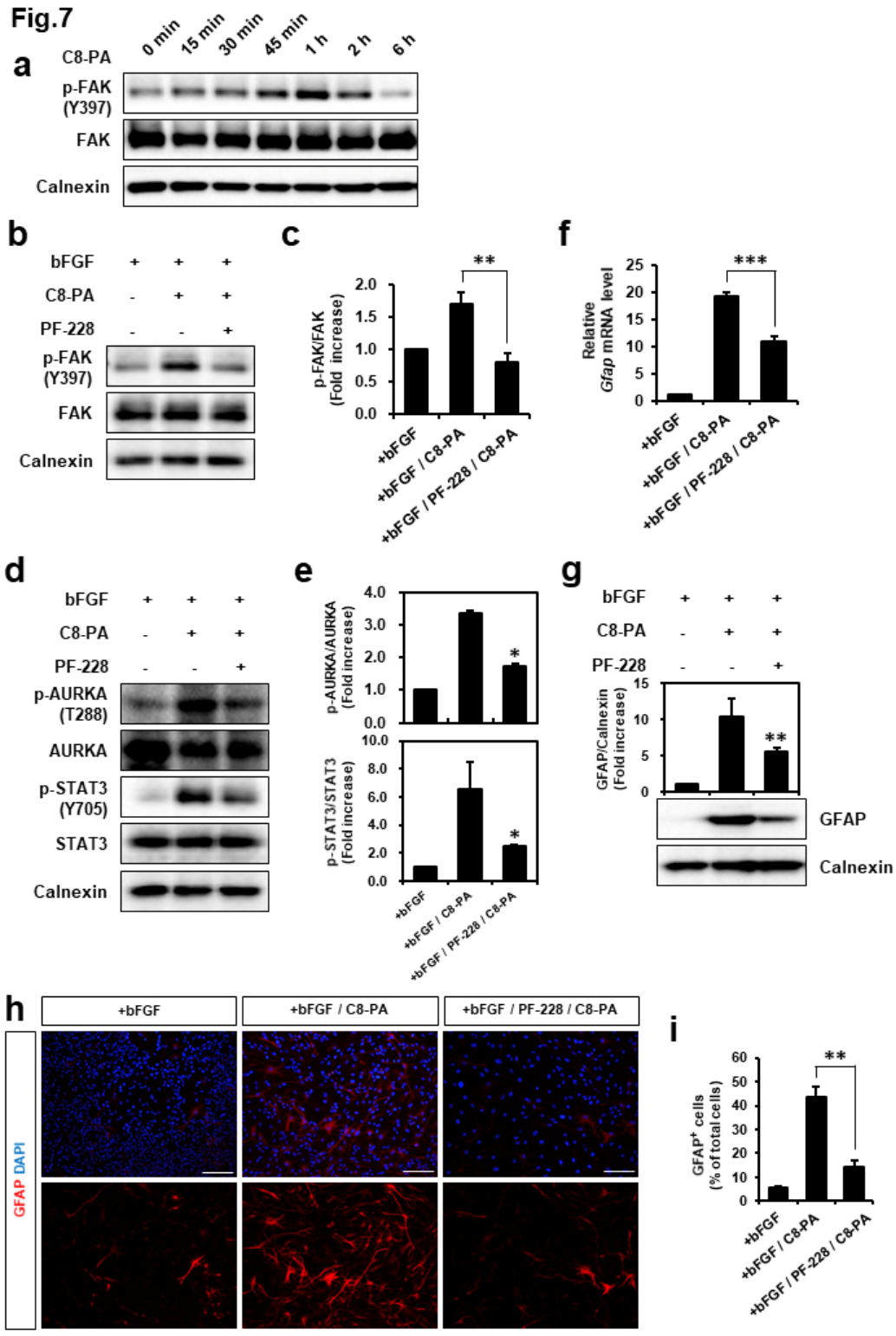

Figure 7

Effect of FAK on AURKA/STAT3 activation during PA-induced astrocytic differentiation of hippocampal NSPCs.

(A) Hippocampal NSPCs were treated with C8-PA (100 μM) for the indicated time durations in the presence of bFGF. Proteins (20 μg) were analyzed by western blotting with anti-phospho-FAK (Tyr397),

anti-FAK, and anti-calnexin antibodies. **(B-C)** Hippocampal NSPCs were pretreated with 5 μM PF-573228 (PF-228) for 2 h and stimulated with C8-PA (100 μM) for 1 h. **(B)** Samples of protein were determined by western blotting using anti-phospho-FAK (Tyr397), anti-FAK, and anti-calnexin antibodies. **(C)** Quantitative analyses of the phosphorylated FAK (Tyr397) level shown in **(B)**. The phosphorylated FAK level was normalized to the total FAK level. Band intensities were quantified using Quantity One® software. Data represent the mean ± SEM of three independent experiments. $^{**}p < 0.01$ compared with the +bFGF/C8-PA. **(D-E)** Cells were pretreated with 5 μM PF-228 for 2 h and treated with C8-PA (100 μM) for 24 h. **(D)** Western blotting was performed using anti-phospho-AURKA (Thr288), anti-AURKA, anti-phospho-STAT3 (Tyr 705), anti-STAT3, and anti-calnexin antibodies to detect the respective protein bands. **(E)** Quantitative analyses of the phospho-AURKA (Thr288) and phosphor-STAT3 (Tyr705) levels shown in **(D)**. Values were normalized to that of the total AURKA or STAT3 level. Band intensities were quantified using Quantity One® software. Data represent the mean ± SEM of three independent experiments. $^{*}p < 0.05$ compared with the +bFGF/C8-PA. **(F-G)** Cells were pretreated with 5 μM PF-228 for 2 h and treated with C8-PA (100 μM) for 72 h. **(F)** *Gfap* mRNA level was measured by real-time RT-PCR. Data represent the mean ± SEM of three independent experiments. $^{***}p < 0.001$ compared with C8-PA-treated cells. **(G)** GFAP and calnexin protein levels were determined by western blotting. GFAP protein level was normalized to the level of calnexin. Band intensities were quantified using Quantity One® software. Data represent the mean ± SEM of three independent experiments. $^{**}p < 0.01$ compared with the +bFGF/C8-PA. (**H-I)** Hippocampal NSPCs were pretreated with 5 μM PF-573228 (PF-228) for 2 h and stimulated with C8-PA (100 μM) for 72 h. **(H)** Fixed cells were stained for immunocytochemical analysis of astrocytic (GFAP, red) markers. Scale bar, 100 μm. **(I)** The proportions of GFAP-positive cells and total cells were determined in randomly selected areas from five slides of each condition. Data are mean ± SEM. $^{**}p < 0.01$ compared with the +bFGF/C8-PA.

Fig.8

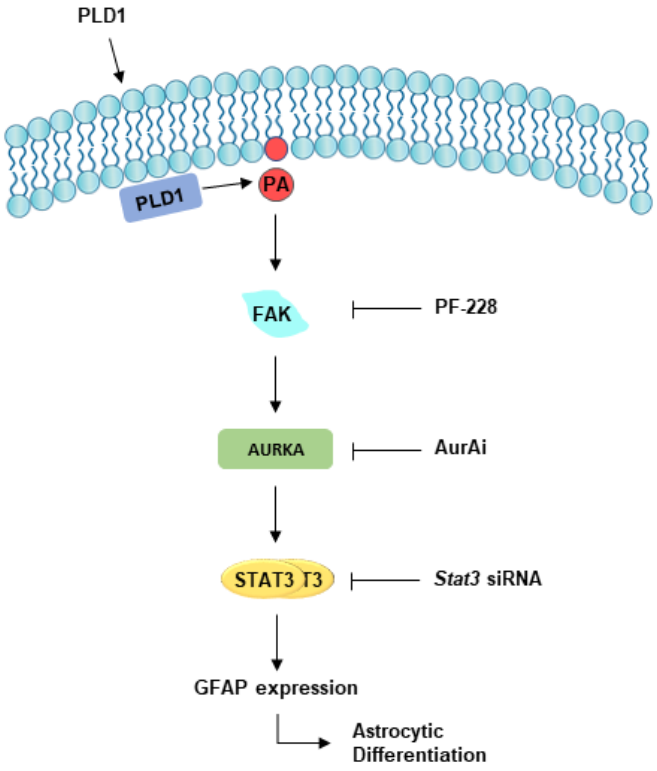

Figure 8

Proposed model for PLD1-induced astrocytic differentiation in hippocampal NSPCs.

The model suggests that PLD1 induces astrocytic differentiation through the PA/FAK/AURKA/STAT3 pathway, leading to increased GFAP expression in hippocampal NSPCs.

Supplementary Files

This is a list of supplementary files associated with this preprint. Click to download.

- SupplementaryMaterial.docx.pdf